

A forming-free bipolar resistive switching behavior based on ITO/V₂O₅/ITO structure

Zhenni Wan, Robert B. Darling, Arka Majumdar, and M. P. Anantram

Citation: *Appl. Phys. Lett.* **111**, 041601 (2017); doi: 10.1063/1.4995411

View online: <http://dx.doi.org/10.1063/1.4995411>

View Table of Contents: <http://aip.scitation.org/toc/apl/111/4>

Published by the [American Institute of Physics](#)

Articles you may be interested in

[Enlarged read window in the asymmetric ITO/HfO_x/TiN complementary resistive switch](#)

Applied Physics Letters **111**, 043501 (2017); 10.1063/1.4995252

[Nanosecond polarization modulation in vanadium dioxide thin films](#)

Applied Physics Letters **111**, 041103 (2017); 10.1063/1.4996361

[Tunable electron affinity with electronic band alignment of solution processed dielectric](#)

Applied Physics Letters **111**, 041602 (2017); 10.1063/1.4995982

[Color mixing from monolithically integrated InGaN-based light-emitting diodes by local strain engineering](#)

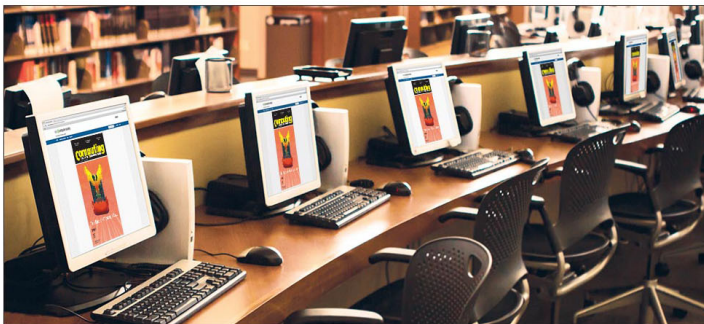
Applied Physics Letters **111**, 041101 (2017); 10.1063/1.4995561

[Deep donor state of the copper acceptor as a source of green luminescence in ZnO](#)

Applied Physics Letters **111**, 042101 (2017); 10.1063/1.4995404

[Enhancement of resistive switching properties in nitride based CBRAM device by inserting an Al₂O₃ thin layer](#)

Applied Physics Letters **110**, 203102 (2017); 10.1063/1.4983465



CiSE is already at
your fingertips...



In the IEEE Xplore and
AIP library packages.

A forming-free bipolar resistive switching behavior based on ITO/V₂O₅/ITO structure

Zhenni Wan,^{a)} Robert B. Darling, Arka Majumdar, and M. P. Anantram

Department of Electrical Engineering, University of Washington, Seattle, Washington 98105, USA

(Received 6 April 2017; accepted 11 July 2017; published online 24 July 2017)

Forming-free bipolar resistive switching behavior in an ITO/V₂O₅/ITO structure is observed. While the bottom ITO layer functions as a common ground electrode, the top ITO layer is an active element and used as an oxygen reservoir, with an additional metal electrode patterned on its top for making contact. In contrast to typical metal/transition metal oxide/metal based resistive memories, our device exhibits a low resistance state in its virgin state and is switched to a high resistance state when a forward bias of $\sim +2.5$ V is applied. The device can be reset to its original state at a reverse bias of ~ -1.5 V. A noticeable decrease in switching voltage with a reduced top contact area is observed, indicating a strong electric field enhanced switching mechanism. Different from the widely seen conductive filament mechanism in bipolar switching, we explain the switching behavior by the migration of oxygen ions at the top ITO/V₂O₅ interface. When oxygen ions are extracted to the ITO side, an interfacial layer with reduced oxidation states is formed and acts as a Schottky barrier that suppresses the current through the whole device. The results suggest future applications in low power, high speed integrated non-volatile memories. *Published by AIP Publishing.* [<http://dx.doi.org/10.1063/1.4995411>]

Resistive random access memory (RRAM) is considered as one of the most promising candidates for next generation memory due to its high speed,^{1,2} low power consumption,¹ and superior scalability.^{2,3} Most RRAMs are based on Metal-Insulator-Metal (MIM) systems and can be divided into two categories: unipolar switching and bipolar switching.⁴ The generally accepted physical mechanisms responsible for bipolar switching are the formation and annihilation of conductive filaments due to the migration of ions driven by an electric field.⁵ Prior to resistive switching behavior, a large forming voltage that is a few times higher than the switching voltage is usually required to form the conductive filaments in a pristine insulator layer.⁴ However, such high forming voltages exceeding ± 10 V expose severe electrical and mechanical stresses to the MIM memory element. Dramatic changes in the film morphology are observed after forming, including partial spalling and ablation of the electrode material.⁶ The forming process may also result in unpredictable resistance states, which lowers the device yield.^{7,8} Obviously, reducing or even eliminating the forming step is valuable for practical applications.

So far, the so-called forming-free resistive switching with two different characteristics has been realized. In the first case, the pristine state resistance is similar to the high resistance state (HRS) resistance after reset, and the forming voltage is also comparable with the subsequent set voltage.⁹ In the second case, pre-existing conductive filaments in the as-fabricated RRAM cells result in an initial ON state.¹⁰⁻¹³ However, both cases require elaborate control of defect profiles in the device to be achieved by various approaches, including film thickness optimization,¹¹ ion doping,^{9,12} thermal treatment,¹⁰ and fabrication modulation,^{9,13} which increases the complexity of fabrication. Vanadium pentoxide

(V₂O₅) is widely used as a cathode material for lithium batteries¹⁴⁻¹⁶ due to its layered atomic structure^{17,18} and the capability of storing intercalating ions.¹⁹ Its potential application in resistive memory has not yet been explored. In this work, we demonstrate a forming-free bipolar resistive switching in an ITO/V₂O₅/ITO sandwich structure. Commercial ITO coated glass with a sheet resistance of 15 Ω/sq is used as a substrate and bottom contact. The carrier concentration is estimated to be $9.66 \times 10^{20} \text{ cm}^{-3}$, by using parameters from the literature.²⁰ The Fermi level is thus calculated to be around 1.02 eV above the conduction band minimum.^{21,22} A thin film of V₂O₅ with a thickness of 300 nm is deposited using a sol-gel process. The top layer of ITO (160 nm) is deposited by magnetron sputtering, and the corresponding sheet resistance is 50 Ω/sq . Using a procedure similar to that adopted for the bottom contact, the Fermi level of the top ITO contact is estimated to be 0.50 eV above the conduction band minimum. After the deposition of the top ITO, a post annealing step is applied at 300 °C for 20 min in ambient air to remove the intercalated water molecules in the V₂O₅ xerogel layer. An additional top contact made from Cr (20 nm)/Al (260 nm)/Cr (20 nm) is then deposited and patterned by a shadow mask, with circular contact diameters ranging from 30 μm to 100 μm .

The current-voltage (I-V) characteristics of the device were measured by a custom-built probe station and a Keithley 4200 source meter unit (SMU). The bias voltage is applied on the top metal electrode, and the bottom ITO electrode is grounded. The measured characteristics are shown in Fig. 1. An abrupt drop in current is observed at around +2.5 V, which is reflected in a static resistance that has increased by 3–8 times, and varies with different devices. The current level is reset to its original state after a reverse bias of -1.5 V is applied. Subsequent sweeps show consistent and reproducible resistive switching characteristics. Notice

^{a)}Author to whom correspondence should be addressed: jennywan@uw.edu

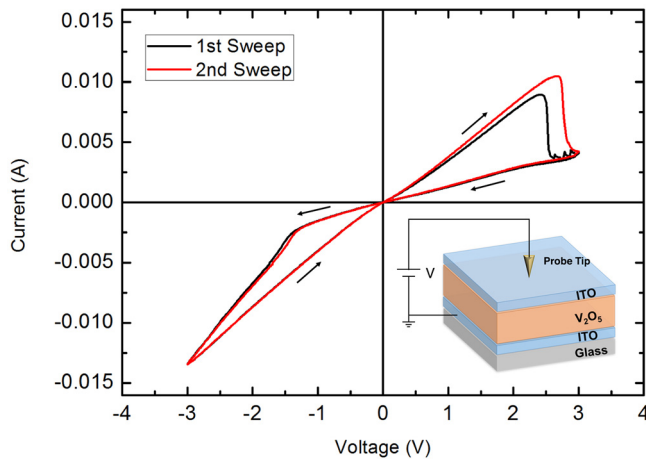


FIG. 1. Resistive switching characteristics of the ITO/ V_2O_5 /ITO structure, measured by using a probe tip ($2\ \mu\text{m}$ diameter) on the top ITO layer. The applied voltage varies from $0\ \text{V} \rightarrow 3\ \text{V} \rightarrow 0\ \text{V} \rightarrow -3\ \text{V} \rightarrow 0\ \text{V}$. Abrupt resistive switching is observed at $+2.5\ \text{V}$ during the initial sweep. The resistance is reset to its initial state after a bias of $-1.5\ \text{V}$ is applied.

that no forming process is required prior to the bipolar switching behavior. During the DC voltage sweep, no current compliance is applied either. The results not only suggest a reversible bipolar resistive memory behavior in the V_2O_5 device but also imply a switching mechanism different from conventional resistive memories with metal-insulator-metal structures, in which case a large forming voltage is required to create conductive filaments in the pristine insulator layer. In addition, the large thickness of the V_2O_5 layer prevents the formation of any conductive filaments bridging two electrodes under such small biases.

Figure 2 shows the transient response of the device to applied voltage pulses with a width of $200\ \text{ns}$ in a full programming and erase cycle. The initial state of the device is read by a $+0.2\ \text{V}$ voltage pulse [Fig. 2(a)], and this shows a high current of $580\ \mu\text{A}$. Then, a $+4\ \text{V}$ pulse is applied, followed by another “read” operation that shows a lowered current of $300\ \mu\text{A}$ [Fig. 2(b)]. A $-4\ \text{V}$ pulse is applied to reset the current of the device to $620\ \mu\text{A}$ [Fig. 2(c)]. The

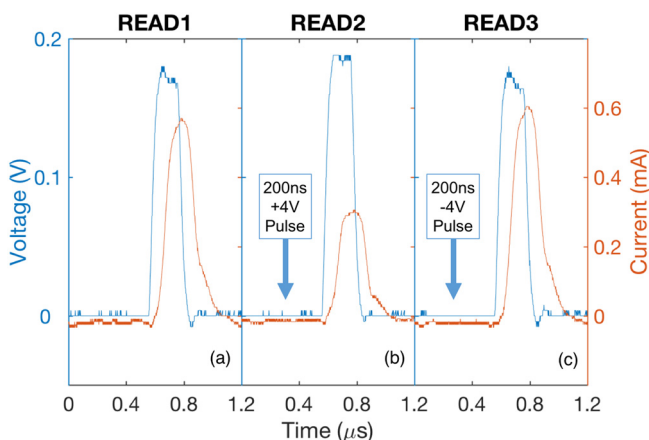


FIG. 2. Transient response of the ITO/ V_2O_5 /ITO device. The applied voltage is shown in blue. The detected current is shown in green. (a) $+0.2\ \text{V}$, $200\ \text{ns}$ “READ” pulse in the low resistance state. (b) $+0.2\ \text{V}$, $200\ \text{ns}$ “READ” pulse in the high resistance state after applying a “SET” pulse of $+4\ \text{V}$, $200\ \text{ns}$. (c) $+0.2\ \text{V}$, $200\ \text{ns}$ “READ” pulse returning to the low resistance state after applying a “RESET” pulse of $-4\ \text{V}$, $200\ \text{ns}$.

transient response results show that the devices have the potential to operate in high speed circuits.

ITO/ V_2O_5 /ITO devices with different metal contact diameters varying from $30\ \mu\text{m}$ to $100\ \mu\text{m}$ were fabricated. Reversible switching characteristics are observed for all the devices but at different voltage biases. A systematic linear drop in the positive switching voltage is found when the contact diameter decreases. The results are shown in Fig. 3. The lowest switching voltage ($+2.5\ \text{V}$) is observed when a probe tip with a diameter of $2\ \mu\text{m}$ is directly in contact with the top ITO layer. A similar trend is also observed for the negative switching voltages.

The results indicate a significant fringe field effect associated with the switching process. As the contact becomes smaller, the electric field beneath the electrode increases due to the larger circumference to area ratio, thus enhancing the migration of mobile ions in the system and reducing the required applied voltage for switching. The contact size dependent switching voltage of the tested devices also supports the hypothesis that the conductive filament mechanism, which generally does not depend on contact size, is unlikely to be the underlying physics of switching.

Irreversible resistive switching characteristics were discovered in V_2O_5 xerogel films sandwiched by chromium electrodes in our previous work.²³ When a sufficient voltage bias is applied, oxygen vacancies formed at V_2O_5/Cr interfaces create an energy barrier for electrons to overcome, thus reducing the conductance of the device. Such a switching process is catalyzed by the intercalated water molecules in the V_2O_5 xerogel film. Oxygen gas is released after switching, and a permanent loss of oxygen ions was proposed to be the reason for the irreversibility.

When the electrodes are replaced by ITO and a post annealing step is added, the reduction in the conductance of the devices becomes reversible. Indium tin oxide has a fluorite structure with 25% empty oxygen sites in an ordered array.²⁴ Unlike the dense chromium electrodes, a conductive ITO film deposited by RF sputtering has oxygen vacancies

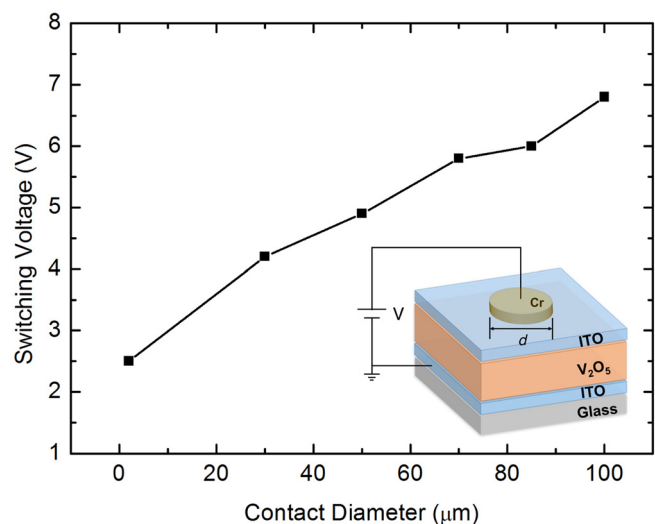


FIG. 3. Positive switching voltage increases approximately linearly with the diameter of the top metal contact. The smallest switching voltage ($+2.5\ \text{V}$) is observed with a probe tip ($\sim 2\ \mu\text{m}$ diameter). The highest switching voltage ($+6.8\ \text{V}$) is observed when the contact diameter is $100\ \mu\text{m}$.

acting as both a source for free electrons and a reservoir for oxygen ions. Yang *et al.*²⁵ reported a bipolar switching behavior in the ITO/HfO₂/ITO system which usually involves conductive filaments consisting of oxygen vacancies. This observation indicates that ITO can store oxygen ions in a reversible way. The post annealing step removes the intercalated water molecules in the V₂O₅ film and thus prevents the formation of oxygen gas. In our experiments here, no bubbles were observed after the reversible switching.

It is proposed that the creation of oxygen vacancies in the V₂O₅ lattice at the V₂O₅/ITO interface is responsible for the resistive switching. When a positive voltage is applied on the top electrode, oxygen ions are extracted from the V₂O₅ lattice and driven to fill in the oxygen vacancies in the top ITO layer, leaving a thin vanadium oxide layer with reduced oxidation states behind. A reduction in electron affinity is expected due to the loss of oxygen,²⁶ and thus, a thin Schottky barrier is formed between the vanadium oxide layer and ITO electrode (Fig. 4). This is also consistent with the experimental observation that the conduction band minimum of V₂O₅ shifts to about 1 eV above the Fermi level when the oxidation state is reduced, while the position of valence band maximum barely changes.²⁷ Before the reduction, the conduction band was only 0.3 eV above the Fermi level. The band gap of ITO is 2.9 eV according to the literature,²⁸ and the position of the Fermi level has been calculated previously. The filling of oxygen vacancies in the ITO layer also results in an increase in the resistance. This corresponds to the abrupt decrease in current in I-V characteristics under forward bias. When a negative voltage is applied, oxygen ions are driven back to refill the vacancies in the interfacial layer, resulting in the conductance increasing back to its initial state.

Although the ITO/V₂O₅/ITO device structure seems to be symmetrical, asymmetry in electrical properties is observed when a reverse sweep is applied first. No resistive

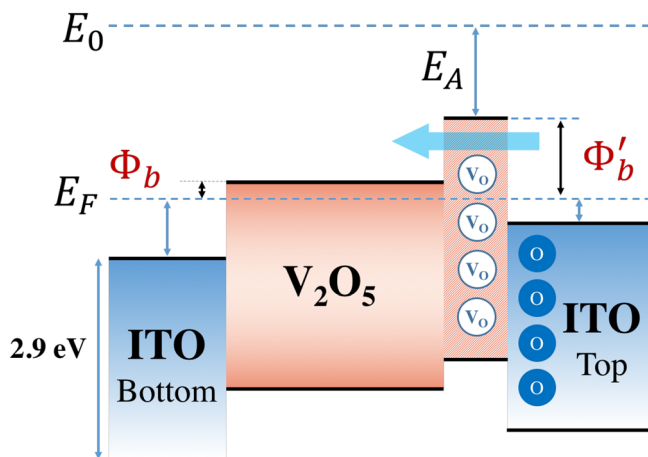


FIG. 4. Proposed band diagram of the ITO/V₂O₅/ITO structure after a “SET” operation. At the top ITO/V₂O₅ interface, oxygen ions migrate from the V₂O₅ side to the ITO side, leaving an interfacial vanadium oxide layer with reduced oxidation states. A thin Schottky barrier is formed due to the reduced electron affinity of the interfacial layer, which is responsible for the increased resistance. Oxygen ions can be driven back into V₂O₅ when a negative voltage is applied.

switching occurs up to -4 V, and the I-V characteristics of the device remain resistor-like. The switching appears only when a forward (positive) bias is applied to the top electrode. This observation implies that oxygen ions do not migrate at the bottom V₂O₅/ITO interface, and the two interfaces are asymmetric. We believe that the asymmetry originates from different fabrication processes for the ITO layers. The bottom V₂O₅/ITO interface is formed in a sol-gel process that does not involve high-energy irradiation. When the top ITO is deposited on the V₂O₅ film, the whole substrate is immersed in an argon plasma, and it is possible that the surface lattice structure of the V₂O₅ film has changed to a more reactive state after this exposure. Another possible explanation is the asymmetrical contact size. The bottom ITO electrode covers the whole wafer and is much bigger than the top metal contact. When a reverse bias is applied, the electric field is less confined at the bottom V₂O₅/ITO interface, making ion migration more difficult to occur.

To investigate the robustness of the resistive switching behavior, we have measured current-voltage characteristics at temperatures varying from 4.0 °C to 62.3 °C (Fig. 5). Distinct switching features can be observed at all the temperatures tested without degradation, showing that the device has potential to operate in a wider temperature range.

Preliminary endurance cycling tests of the device have also been performed in ambient air conditions at room temperature (results not listed). After about 10 cycles, destructive changes of the surface topography are observed, resulting in the degradation of the top contact. The LRS and HRS can then no longer be detected due to a high contact resistance. Future engineering of the film quality and fabrication process will be needed to solve this issue.

In summary, reversible bipolar resistive switching is observed in a metal/ITO/V₂O₅/ITO structure. Opposite to the conventional bipolar switching observed in MIM structures, the device starts with a low resistance state (LRS) and is switched to a high resistance state (HRS) without a prior forming process when a positive voltage is applied on the top electrode. The switching voltage decreases when the size

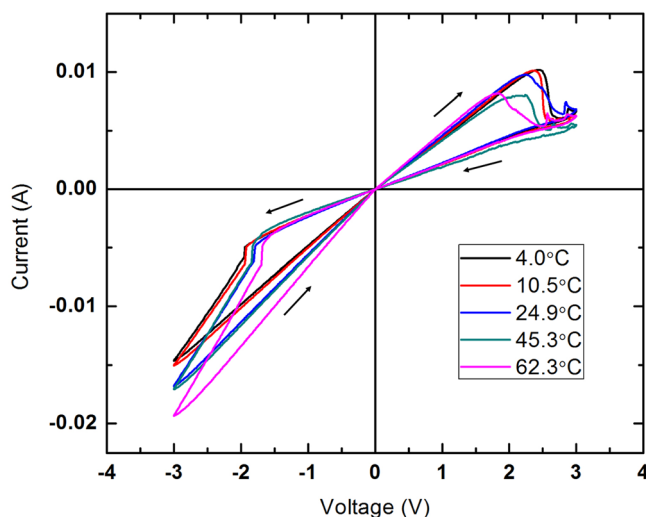


FIG. 5. Current-voltage characteristics of the ITO/V₂O₅/ITO structure at different temperatures varying from 4.0 °C to 62.3 °C. Resistive switching behavior persists in the tested temperature range.

of the top metal contact is reduced, indicating a significant fringe effect that enhances the electric field beneath the contact and thus accelerates the migration of oxygen ions at the top ITO/V₂O₅ interface. Creation of oxygen vacancies in the vanadium oxide layer and filling of oxygen vacancies in the ITO layer are responsible for the increased resistance after switching. The results suggest future applications of this V₂O₅ structure in low-power, high speed integrated non-volatile memories.

The authors would like to thank Washington Nanofabrication Facility (WNF) and EE Micro Fabrication Laboratory for the help with device fabrication and characterization. We also thank EE Nanophotonics Lab for support with measuring the transient response.

- ¹H. Y. Lee, P. S. Chen, T. Y. Wu, Y. S. Chen, C. C. Wang, P. J. Tzeng, C. H. Lin, F. Chen, C. H. Lien, and M. J. Tsai, in *Electron Device Meeting, 2008. IEDM 2008. IEEE Int.* (IEEE, 2008), pp. 1–4.
- ²Y. C. Yang, F. Pan, Q. Liu, M. Liu, and F. Zeng, *Nano Lett.* **9**, 1636 (2009).
- ³B. Govoreanu, G. S. Kar, Y. Y. Chen, V. Paraschiv, S. Kubicek, A. Fantini, I. P. Radu, L. Goux, S. Clima, and R. Degraeve, in *Electron Device Meeting, 2011. IEDM 2011. IEEE Int.* (IEEE, 2011), pp. 31.6.1–31.6.4.
- ⁴H.-S. P. Wong, H.-Y. Lee, S. Yu, Y.-S. Chen, Y. Wu, P.-S. Chen, B. Lee, F. T. Chen, and M.-J. Tsai, *Proc. IEEE* **100**, 1951 (2012).
- ⁵J. J. Yang, M. D. Pickett, X. Li, D. A. A. Ohlberg, D. R. Stewart, and R. S. Williams, *Nat. Nanotechnol.* **3**, 429 (2008).
- ⁶R. Münstermann, J. J. Yang, J. P. Strachan, G. Medeiros-Ribeiro, R. Dittmann, and R. Waser, *Phys. Status Solidi RRL* **4**, 16 (2010).
- ⁷D. Lee, D.-J. Seong, H. J. Choi, I. Jo, R. Dong, W. Xiang, S. Oh, M. Pyun, S.-O. Seo, and S. Heo, in *Electron Device Meeting, 2006. IEDM 2006. IEEE Int.* (IEEE, 2006), pp. 1–4.

- ⁸D.-H. Kwon, K. M. Kim, J. H. Jang, J. M. Jeon, M. H. Lee, G. H. Kim, X.-S. Li, G.-S. Park, B. Lee, and S. Han, *Nat. Nanotechnol.* **5**, 148 (2010).
- ⁹Z. Fang, H. Y. Yu, X. Li, N. Singh, G. Q. Lo, and D. L. Kwong, *IEEE Electron Device Lett.* **32**(4), 566 (2011).
- ¹⁰M. Kawai, K. Ito, N. Ichikawa, and Y. Shimakawa, *Appl. Phys. Lett.* **96**, 072106 (2010).
- ¹¹Y.-S. Chen, H.-Y. Lee, P.-S. Chen, T.-Y. Wu, C.-C. Wang, P.-J. Tzeng, F. Chen, M.-J. Tsai, and C. Lien, *IEEE Electron Device Lett.* **31**, 1473 (2010).
- ¹²B. Tulu, W. Z. Chang, J. P. Chu, and S. F. Wang, *Appl. Phys. Lett.* **103**, 252904 (2013).
- ¹³X. Cao, X. Li, X. Gao, W. Yu, X. Liu, Y. Zhang, L. Chen, and X. Cheng, *J. Appl. Phys.* **106**, 073723 (2009).
- ¹⁴S. H. Ng, S. Y. Chew, J. Wang, D. Wexler, Y. Tourmayre, K. Konstantinov, and H. K. Liu, *J. Power Sources* **174**, 1032 (2007).
- ¹⁵A.-M. Cao, J.-S. Hu, H.-P. Liang, and L.-J. Wan, *Angew. Chem. Int. Ed.* **44**, 4391 (2005).
- ¹⁶J. Liu, H. Xia, D. Xue, and L. Lu, *J. Am. Chem. Soc.* **131**, 12086 (2009).
- ¹⁷V. Petkov, P. N. Trikalitis, E. S. Bozin, S. J. L. Billinge, T. Vogt, and M. G. Kanatzidis, *J. Am. Chem. Soc.* **124**, 10157 (2002).
- ¹⁸R. Enjalbert and J. Galy, *Acta Crystallogr. Sect. C* **42**, 1467 (1986).
- ¹⁹Y. L. Cheah, V. Aravindan, and S. Madhavi, *J. Electrochem. Soc.* **159**, A273 (2012).
- ²⁰O. Tuna, Y. Selamet, G. Aygun, and L. Ozyuzer, *J. Phys. D: Appl. Phys.* **43**, 055402 (2010).
- ²¹I. Hamberg and C. G. Granqvist, *J. Appl. Phys.* **60**, R123 (1986).
- ²²Y. Gassenbauer, R. Schafranek, A. Klein, S. Zafeiratos, M. Hävecker, A. Knop-Gericke, and R. Schlögl, *Phys. Rev. B* **73**, 245312 (2006).
- ²³Z. Wan, R. B. Darling, and M. P. Anantram, *Phys. Chem. Chem. Phys.* **17**, 30248 (2015).
- ²⁴O. N. Mryasov and A. J. Freeman, *Phys. Rev. B* **64**, 233111 (2001).
- ²⁵P.-K. Yang, C.-H. Ho, D.-H. Lien, J. R. Durán Retamal, C.-F. Kang, K.-M. Chen, T.-H. Huang, Y.-C. Yu, C.-I. Wu, and Jr.-H. He, *Sci. Rep.* **5**, 15087 (2015).
- ²⁶H.-J. Zhai and L.-S. Wang, *J. Chem. Phys.* **117**, 7882 (2002).
- ²⁷J. Meyer, K. Zilberberg, T. Riedl, and A. Kahn, *J. Appl. Phys.* **110**, 033710 (2011).
- ²⁸A. Walsh, J. L. F. Da Silva, S.-H. Wei, C. Körber, A. Klein, L. F. J. Piper, A. DeMasi, K. E. Smith, G. Panaccione, and P. Torelli, *Phys. Rev. Lett.* **100**, 167402 (2008).